Hindawi Publishing Corporation
Journal of Nanomaterials
Volume 2016, Article ID 4804271, 8 pages
http://dx.doi.org/10.1155/2016/4804271

Research Article

Effect of Aminosilane Modification on Nanocrystalline Cellulose Properties

Nurul Hanisah Mohd,[1] Nur Farahein Hadina Ismail,[1] Johan Iskandar Zahari,[1] Wan Farahhanim bt Wan Fathilah,[1] Hanieh Kargarzadeh,[1,2] Suria Ramli,[1,2] Ishak Ahmad,[1,2] Mohd Ambar Yarmo,[1] and Rizafizah Othaman[1,2]

[1]*School of Chemical Sciences and Food Technology, Universiti Kebangsaan Malaysia (UKM), 43600 Bangi, Selangor, Malaysia*
[2]*Polymer Research Center, Faculty of Science and Technology, Universiti Kebangsaan Malaysia (UKM), 43600 Bangi, Selangor, Malaysia*

Correspondence should be addressed to Rizafizah Othaman; rizafizah@ukm.edu.my

Received 27 May 2016; Revised 26 July 2016; Accepted 27 July 2016

Academic Editor: Zeeshan Khatri

The application of renewable nanomaterials, like nanocrystalline cellulose (NCC), has recently been widely studied by many researchers. NCC has many benefits such as high aspect ratio, biodegradability, and high number of hydroxyl groups which offer great opportunities for modification. In this study, the NCC derived from empty fruit bunches (EFB) was modified with aminosilane, 3-(2-aminoethylamino)propyl-dimethoxymethylsilane (AEAPDMS), and the characterization was performed to investigate the potential as carbon dioxide (CO_2) capture. Modification of NCC with AEAPDMS was carried out in water/ethanol solvent (80/20) (v/v) with a ratio of NCC to aminosilane of 1 : 1, 1 : 2, 1 : 3, and 1 : 4 w/w%. The effects of AEAPDMS on NCC were characterized using Fourier transform infrared (FTIR) spectroscopy, thermogravimetric analysis (TGA), X-ray diffraction (XRD) analysis, elemental analysis (CHNS), and transmission electron microscopy (TEM). The existence of AEAPDMS onto NCC was confirmed by ATR-FTIR spectroscopy as the new peaks of NH_2 were bending and wagging, and Si-CH_3 appeared. The thermal stability of NCC increased after modification due to the interaction with AEAPDMS. The elemental analysis result showed that the nitrogen content increased with an enhancement ratio of the modifiers. The XRD indicated that the crystallinity decreased while the rod-like geometry of NCC was maintained after amorphous AEAPDMS grafted on the NCC. Since AEAPDMS can be grafted on the NCC, the sample is applicable as CO_2 capture.

1. Introduction

Oil palm production is a major agricultural industry and recently there are more than three million hectares of oil palm plantations in Malaysia [1]. Oil palm empty fruit bunches fibers (OPEFB) represent about 9% of this total, as they are left unutilized after the fruit bunches are pressed at oil mills and the oil is extracted. OPEFB consist of 44.4% cellulose, 30.9% hemicellulose, and 14.2% lignin and are still considered an underutilized resource [2, 3]. Cellulose is available in various types of natural fibers such as wood, cotton, jute fiber, and pineapple fiber [4] but, recently, the abundant waste of natural fiber become a famous topic for researchers [5]. Cellulose is a semicrystalline polysaccharide appearing in nature in the form of fibers [6] and consists of a linear homopolysaccharide composed of β-D-glucopyranose units linked together by β-1-4-linkages like shown in Figure 1 [7–9].

Nanotechnology refers to the concepts and techniques used to make products with unique functionality based on their nanoscale properties. Nanomaterials have great potential for a vast range of applications including medicine, electronics, biomaterials, and energy storage/production. A promising family of renewable nanomaterials is, nonetheless, in the form of nanofibrillated cellulose (NFC), nanocrystalline cellulose (NCC), and bacterial cellulose (BC). These polysaccharide nanoparticles can be obtained from cellulose, the most abundant renewable form of biomass in nature [10, 11]. Nanocellulose has great potential for applications

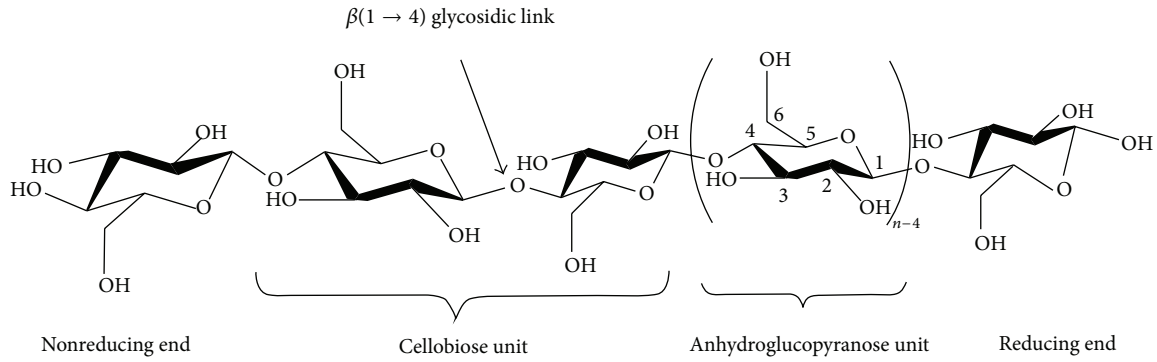

Figure 1: The structure of polymer of cellulose chain shows the anhydroglucose unit in the chair conformation along with atom numbering and the glycosidic link as well as both reducing and nonreducing ends of the polymer.

of coatings, polymer composites, and absorbents/adsorbents and as rheological modifiers or emulsifiers. Nanocellulose has many advantages like low cost, biodegradability, and chemically reactive surface functionality [10].

Among the nanosized cellulose, NCC or nanocrystalline cellulose which is produced by acid hydrolysis from cellulose fibers arose much interest [10, 12, 13]. A complete dissolution of the noncrystalline fractions yields rod-like nanocrystals with 5 to 20 nm in width and up to 1 μm in length, depending on the source of cellulose, and the exact hydrolysis conditions [12, 14]. Compared to cellulose fibers, NCC possesses many advantages, such as nanoscale dimension, high specific strength, high aspect ratio, modulus, and surface area [10, 15, 16]. The feasibility of nano- and microcelluloses is further promoted by their large surface area, chemical accessibility, and functional flexibility [17]. The NCC morphology depends on cellulose source and the preparation conditions such as type and concentration of acid, acid-to-cellulose ratio, reaction time, and temperature [18, 19]. When prepared in sulphuric acid, they possess negative charges on their surface due to the formation of sulfate ester groups during acid treatment, which enhances their stability in aqueous solutions. According to its structure, NCC possesses an abundance of hydroxyl groups on the surface, where chemical reactions can be conducted [11]. The OH group of the sixth position acts as a primary alcohol among the three kinds of hydroxyl groups, where the modification mostly occurs [20].

Many reactions can be used to modify the surface of nanocellulose such as using coupling agents, that is, silane reagents [6]. The interactions of silane coupling agents with natural fibers are widely known [21] and the modification involves polymerization on the NCC surface [7]. Aminosilanes containing primary, secondary, and tertiary amines are silane reagents that have been used for cellulose modification. According to [22], they have a hydrolytically sensitive center that can react with hydroxyl groups or silanols to form a silylated surface. Gebald et al. [23] introduced amine-based adsorbents for air capture by synthesizing and grafting them onto NFC supports. Lu et al. [24] had also grafted aminosilanes onto NFC for epoxy composite applications. 3-(2-Aminoethylamino)propyl-dimethoxymethylsilane

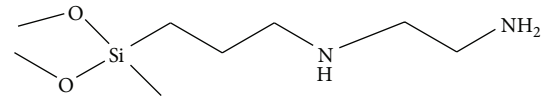

Figure 2: 3-(2-Aminoethylamino)propyl-dimethoxymethylsilane (AEAPDMS) structure.

(AEAPDMS) as shown in Figure 2 is a known silane reagent which has been used by many researchers to modify NFC and MCM-41 for carbon dioxide (CO_2) capture. There is still lack of report on utilization of AEAPDMS as a coupling agent modifier with NCC in the production of adsorbent. However, recently few researchers reported that NCC was successfully modified with 3-glycidoxypropyltrimethoxysilane (GPTMS), 3-methacryloxy-propyltrimethoxysilane (MPS) [25], and y-ammnonimpropylmethyldimethoxysilane (APMDS) [26] which improved the compatibility in polyurethane.

In this study, NCC was isolated from OPEFB cellulose by hydrolysis with sulphuric acid. The NCC was further modified with aminosilane, AEAPDMS. The objective of this study is to investigate the characteristics of modified NCC as based material to produce solid adsorbent aerogel for CO_2 adsorption. The physical and morphology characters of modified NCC were determined by Fourier transform infrared (FTIR) spectroscopy, thermogravimetric (TGA) analysis, X-ray diffraction spectroscopy (XRD), elemental analysis (CHNS), and transmission electron microscope (TEM).

2. Experimental

2.1. Materials and Methods. Oil Palm Empty Fruit Bunch Fiber (OPEFB) in this study was supplied by Szetech Engineering Sdn. Bhd., Selangor, Malaysia. Chemicals used for extraction of cellulose were sodium hydroxide (NaOH), ethanol, toluene, sodium chlorite ($NaClO_2$), and glacial acetic acid, while the chemical used for hydrolysis was sulphuric acid (H_2SO_4). Chemicals used for modifications were 3-(2-aminoethylamino)propyl-dimethoxymethylsilane (AEAPDMS), from Germany, and acetic acid. All chemicals were purchased from Sigma Aldrich, USA.

2.2. Preparation and Modification of Nanocrystalline Cellulose (NCC). The OPEFB fiber was treated by soxhlet extraction, alkali treatment (4% NaOH solution), and bleaching treatment to remove lignin and hemicellulose until the white cellulose was obtained [21, 27, 28]. Then, the NCC was isolated by the method adopted from [21] with slight modifications; that is, acid hydrolysis was conducted at 60% of aqueous H_2SO_4 for 40 minutes at 45°C under mechanical stirring. The NCC suspension was centrifuged, dialysed against distilled water until a constant pH was maintained, and then preserved and stored in refrigerator. The methods of modification of NCC were referred to Abdelmouleh et al. [29], Xie et al. [30], and Bendahou et al. [12] with slight alterations. The modification was carried out in 80/20 (v/v) water/ethanol solvent. The liquid of AEAPDMS (1, 2, 3, and 4 w/w%) was added into the mixture and stirred. The pH of the solution was adjusted to pH 4 by adding few drops of acetic acid and stirred continuously for 1 hour. The pH was maintained at pH 4 since the hydrolysis rate of silanes forming silanol is higher than the condensation rate [26, 30]. Then, 1 w/w% of NCC suspensions were mixed in the solution and refluxed for 3 hours at 60°C by mechanical stirrer. After 3 hours, the heat was turned off and continuously stirred overnight. The NCC-AEAPDMS solution was centrifuged to remove the excess AEAPDMS that did not graft on the NCC; then the NCC and NCC-AEAPDMS samples were freeze-dried for 24 hours before being characterized under various analyses. However, the NCC and NCC-AEAPDMS for TEM analysis were kept in aqueous suspension.

2.3. Characterization

2.3.1. Elemental Analysis (CHNS). The elemental analysis was carried out to investigate the total content of elements in the NCC sample after modification and was performed by using LECO CHNS-932 elemental analyzer. The carbon, hydrogen, nitrogen, and sulphur content of unmodified and modified NCC samples were measured independently.

2.3.2. Attenuated Total Reflectance-Fourier Transform Infrared Spectroscopy (ATR-FTIR). The NCC and NCC-AEAPDMS with a few ratios were analyzed with a Perkin Elmer Spectrometer (spectrum 400 FT-IR) using attenuated total reflectance (ATR) as analysis method. The spectra obtained were recorded in the range 400–4000 cm^{-1}.

2.3.3. Thermogravimetric (TGA) Analysis. Thermal stability of modified NCC and NCC samples was determined by thermogravimetric analyzer (Mettler Toledo model TGA/SDTA851e). The analysis was conducted with temperature in the range 25 to 600°C at 10°C/min heating rate.

2.3.4. X-Ray Diffraction (XRD). The crystallinity in the sample was analyzed using Bruker AXS X-ray diffraction, Germany (model D8 advance), generated at 40 kV and 40 mA. Monochromatic CuKα was used for radiation at wavelength 0.154 nm. The crystallinity index (CrI) was calculated from each sample by using the following equation which was introduced by Segal et al. [31]:

$$\text{CrI } (\%) = \frac{I_{002} - I_{\text{am}}}{I_{002}} \times 100\%, \quad (1)$$

where I_{002} is the maximum intensity of crystallinity of diffraction peak and I_{am} is the intensity scattered by amorphous part of the sample.

2.3.5. Transmission Electron Microscopy (TEM). Aqueous suspensions (0.1 w/w%) of both the NCC and aminosilane modified NCC were prepared for TEM analysis. A drop of aqueous suspension was deposited on a Cu grid covered with a thin carbon film. The suspension was negatively stained with 2 w/w% uranyl acetate in order to enhance contrast. The morphology of the NCC and modified NCC was observed by using a Philips CM30 microscope operated at an accelerating voltage of 100 kV.

Table 1: Elemental analysis of NCC and aminosilane grafted on NCC.

Materials	Elemental analysis (%)			
	C	H	N	S
NCC	40.28	7.40	—	0.405
NCC-AEAPDMS (1 : 1)	37.46	6.556	0.262	0.625
NCC-AEAPDMS (1 : 2)	41.08	6.535	0.446	0.563
NCC-AEAPDMS (1 : 3)	42.50	6.698	0.767	0.517
NCC-AEAPDMS (1 : 4)	42.65	6.532	0.763	0.519

3. Results and Discussion

3.1. Elemental Analysis (CHNS). Elemental analysis was carried out to confirm the presence of aminosilane grafted on NCC surface. The weight contents of carbon (C), hydrogen (H), nitrogen (N), and sulphur (S) were measured and the results are shown in Table 1. The elemental analysis of unmodified NCC and aminosilane grafted on NCC showed that there was an increment in carbon and nitrogen contents of the sample after modification. The introduction of amine groups on the NCC surface increased the carbon and nitrogen contents [17].

3.2. Fourier Transform Infrared Spectroscopy (FTIR). The effects of introducing AEAPDMS on NCC surface were studied by FTIR analysis like shown in Figure 3. Figure 3(a) is the spectrum for AEAPDMS. NCC spectrum (Figure 3(b)) displayed O-H stretching at 3335 cm^{-1}, C-H stretching at 2900 cm^{-1}, CH_2 bending at 1430 cm^{-1}, and C-O-C skeletal vibrations at 1055 cm^{-1}, while O-H and C-H bending along with C-C and C-O stretching located at 1380, 1317, and 1258 cm^{-1}, respectively. All the peaks are the typical peaks of cellulose [23, 32]. For NCC modified AEAPDMS (Figures 3(c)–3(f)), all spectra showed the emerging of small new peaks located at approximately 1600 cm^{-1} and 798 cm^{-1} which are attributed to NH_2 bending and NH_2

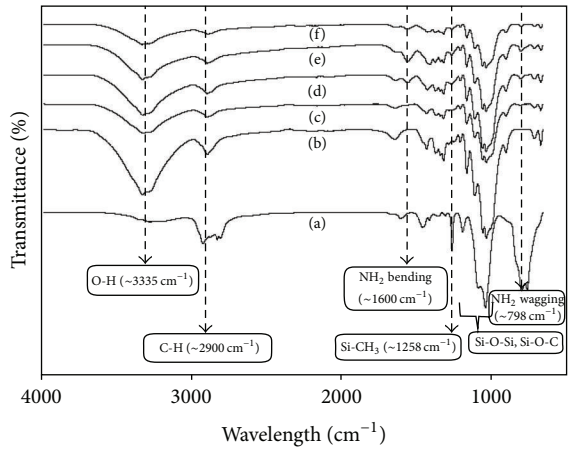

Figure 3: FTIR spectra of (a) AEAPDMS, (b) NCC, and NCC-AEAPDMS with several ratios: (c) 1 : 1 (w/w)%, (d) 1 : 2 (w/w)%, (e) 1 : 3 (w/w)%, and (f) 1 : 4 (w/w)%.

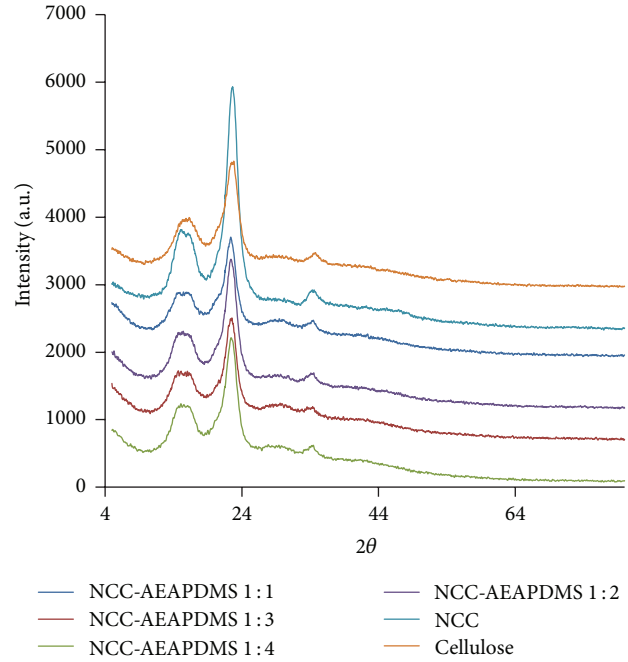

Figure 4: XRD analysis for NCC and all samples of modified NCC.

wagging, respectively. The same peaks that were reported by Abdelmouleh et al. [29] and Zhao et al. [33] are showing that the peaks are typical for the deformation modes of the NH_2 groups of hydrogen bonded to the OH functions of both silanol moieties and cellulosic substrates. Moreover, the high intensity peak of Si-CH_3 at 1258 cm^{-1} as presented in AEAPDMS spectrum was also observed in NCC-AEAPDMS spectra with ratios 1 : 2, 1 : 3, and 1 : 4 around 1260 cm^{-1}, respectively, while the peak was not apparent for 1 : 1 w/w% NCC-AEAPDMS which might be due to the small amount of AEAPDMS added. Bands for -Si-O-Si and -Si-O-C bond at 1160 cm^{-1} and 1104 cm^{-1}, respectively, were overlapped with band C-O-C skeletal vibration in the range 970–1250 cm^{-1}. Rachini et al. [34] reported that the bands detected around 1030, 1055, 1110, and 1146 cm^{-1} were the characteristic bands of the Si-O-Si linkage and Si-O- cellulose. Thus, the existence of all the new peaks of the NCC spectrum indicated that the AEAPMDS was grafted to the O-H functional group on NCC surface.

Based on the FTIR result, it can be seen that AEAPDMS grafted on NCC. The possible reactions are as follows:

$$\begin{aligned} &NH_2CH_2\text{-}Si\text{-}CH_3\,(OCH_3)_2 + H_2O \\ &\quad\longrightarrow NH_2CH_2\text{-}Si\text{-}CH_3\,(OH)_2 + 2CH_3OH \end{aligned} \tag{2}$$

$$\begin{aligned} &NH_2CH_2\text{-}Si\text{-}CH_3\,(OH)_2 + NCC\text{-}OH \\ &\quad\longrightarrow NH_2CH_2\text{-}Si\text{-}CH_3OH\text{-}O\text{-}NCC + H_2O \end{aligned} \tag{3}$$

In this case, the alkoxysilanes does not react directly with hydroxyl (-OH) group of cellulose to form -Si-O-C- even at high temperature. It is attributed to lower acidity of the cellulosic hydroxyl group compared with silanol. Cellulose is generally unreactive to many chemicals and the OH groups of the microfibrils have very low accessibility. Based on former works, an optional strategy was to activate the alkoxysilane by hydrolyzing the alkoxy groups off, forming more reactive silanol groups, and can be further dehydrated with surface hydroxyl groups of cellulose [17, 18, 30]. She et al. [26] reported the same phenomena where the hydroxyl group of the original NCC was replaced by alkyl-oxygen group which was obtained from silanol group via hydrolysis. Rachini et al. [34] soaked sisal fiber in alcoholic solution of aminosilane at a pH between 4.5 and 5.5 to hydrolyze the coupling agent. Valadez-Gonzalez et al. [35] and Agrawal et al. [36] modified henequen and oil palm fiber with a silane solution in a water/ethanol mixture. That is why, in this study, AEAPDMS was hydrolyzed at pH 4 and then modified under a water/ethanol mixture to ensure that the grafting will follow reactions (2) and (3).

3.3. X-Ray Diffraction (XRD). Figure 4 shows the XRD diffractograms of cellulose, NCC, and NCC-AEAPDMS samples. All the diffractograms displayed that the typical peaks of semicrystalline materials consist of broad hump amorphous region and sharp intense peak of crystalline region [21, 37]. Cellulose diffractogram showed three peaks around 2θ = 16°, 22.5°, and 34.5° which are related to the typical type of cellulose I and corresponding to the crystallographic planes that are (101), (002), and (040) [3, 27, 38]. At NCC diffractogram, the peaks at 2θ = 22.5° are getting sharper and more intense showing that the sample is more crystalline. The peak is used to relate to the crystallinity of the materials as can be used to calculate the crystallinity index (CrI) as shown by (1) [39].

Table 2 is crystallinity index (CrI) of all the samples. The cellulose extracted from EFB fiber has the CrI of approximately 64.0%. The CrI of NCC increased to 76.8% after acid hydrolysis by sulphuric acid (H_2SO_4) due to the removal of some amorphous region in cellulose and reducing the size to nano [40]. NCC sample with AEAPDMS showed lower CrI compared to the NCC since AEAPDMS is amorphous

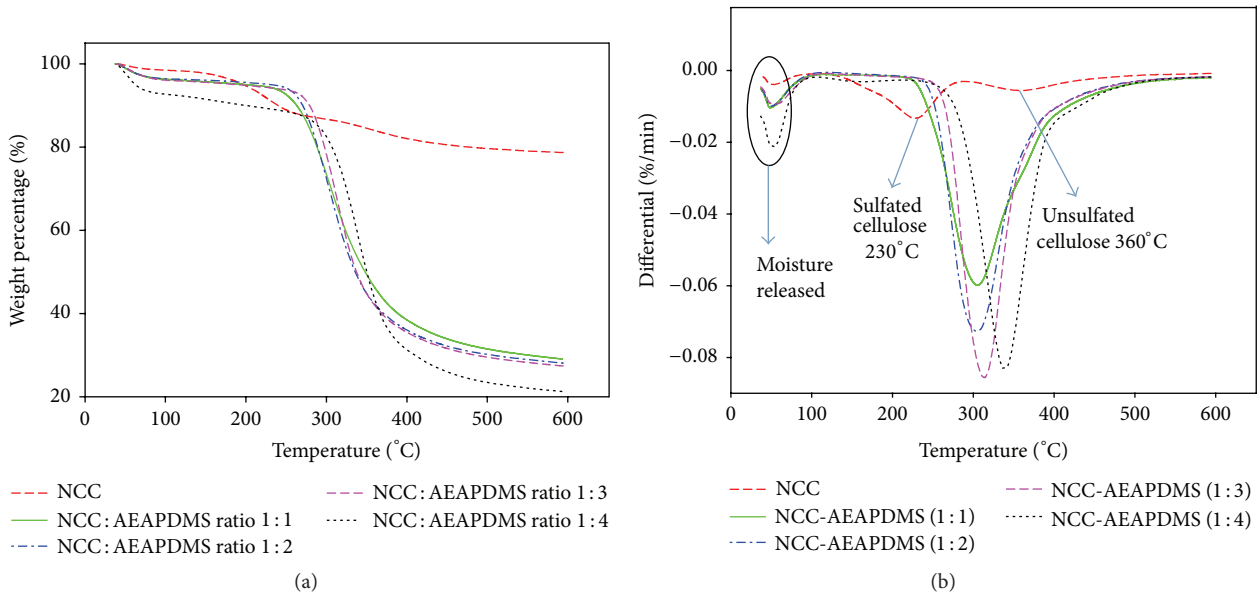

Figure 5: (a) TGA result; (b) DTG result for sample NCC and all samples of modified NCC.

Table 2: Percentage of crystallinity index for unmodified and modified NCC-AEAPDMS.

Sample	Crystallinity index, CrI (%)
Cellulose	64.0
NCC	76.8
NCC-AEAPDMS (1 : 1)	61.6
NCC-AEAPDMS (1 : 2)	66.7
NCC-AEAPDMS (1 : 3)	64.0
NCC-AEAPDMS (1 : 4)	65.1

and being grafted onto the NCC, which increased the total amorphous region and thus reduced the CrI. The replacement of the hydroxyl groups by the amino groups and hydrocarbon chains of silane resulted in the slight degeneration of the compact crystalline regions of NCC during the surface modification. However, there is no trend of CrI reduction with respect to the amount showing that the grafting occurred randomly in both crystalline and amorphous regions of NCC. The decrement of the crystallinity for modified NCC had also been observed by Tian et al. [41] and Zhang et al. [42].

3.4. Thermogravimetric Analysis (TGA). Figures 5(a) and 5(b) show the thermogravimetric analysis (TGA) and differential thermogravimetric (DTG) curves for NCC and NCC modified AEAPDMS. The weight loss was measured in the temperature range of 35 to 600°C. All samples showed that the initial weight loss around 100°C was caused by water evaporation from the samples [28]. The NCC peak consists of two decomposition peaks started at 120°C and later at 300°C. Consequently, the DTG curves displayed the two degradation peaks at the maximum of 230°C and 360°C. Kargarzadeh et al. [21] also reported the two degradation peaks for NCC from acid hydrolysis and discussed that the former is due to highly sulfated amorphous cellulose and the latter is due to breakdown of unsulfated crystals cellulose. However, the TGA curves for modified NCC-AEAPDMS showed the decomposition trends similar to cellulose. This is expected since the CrI of NCC-AEAPDMS was similar to cellulose which indicated that the crystalline and amorphous parts are almost equal. The DTG curves for modified NCC-AEAPDMS showed that the weight loss shifted to a higher temperature and the maximum is around 300–340°C. The thermal stability increased because silane modification on NCC resulted in interaction between NCC and AEAPDMS, thus improving the thermal stability of NCC. Furthermore, AEAPDMS decomposed at higher temperature of 370°C [33]. Wang et al. [43] reported the same trend when treating sisal fibers with silane. The DTG curves NCC-AEAPDMS at ratio of 1 : 4 w/w% showed the highest peak at 340°C compared with ratios of 1 : 1, 1 : 2, and 1 : 3 w/w%. Thus, from thermogravimetric (TGA) analysis, it was determined that the thermal stability of modified NCC improved after aminosilane grafting.

3.5. Transmission Electron Microscope (TEM). The surface morphology of NCC and modified NCC-AEAPDMS at a ratio of 1 : 3 w/w% was studied by TEM as shown in Figure 6. The NCC showed the rod-like shape since H_2SO_4 removed the amorphous part in the cellulose. The effect of H_2SO_4 includes the introduction of negatively charged sulfate group that allows the nanocrystalline NCC to disperse in water [14, 44]. However, there is still some agglomerates due to the hydrogen-bonding interactions between the hydroxyl groups on the NCC surfaces even after sonication process. The phenomenon was also reported by Chen et al. [45] and Kaushik et al. [19]. The NCC particles maintained their rod-like morphology even after the modification with AEAPDMS. The rod-like or needle-shaped acid-hydrolyzed

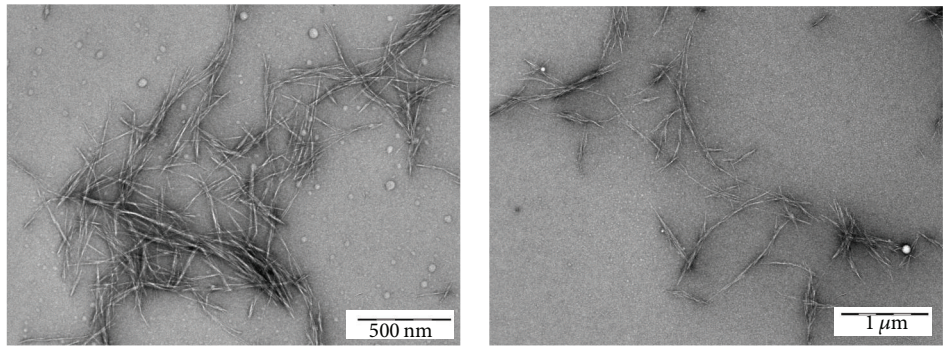

(a) (b)

Figure 6: TEM images of (a) nanocrystalline cellulose (NCC) of OPEFB cellulose and (b) modified NCC-AEAPDMS with a ratio 1 : 3 w/w%.

Table 3: The geometric dimensions of NCC and NCC-AEAPDMS at ratio of 1 : 3 w/w%.

Sample	Length, L (nm)	Width, D (nm)	Aspect ratio (L/D)
NCC	173 ± 0.6	9 ± 0.5	18 ± 0.2
NCC-AEAPDMS (1 : 3)	193 ± 0.9	10 ± 0.4	18 ± 0.6

NCC and modified NCC were characterized by their length (L), width (D), and aspect ratio (L/D) [9] and were tabulated in Table 3. The average dimensions of the nanoparticles NCC were measured and the length was approximately around 173 ± 0.6 nm and width was about 9 ± 0.5 nm. The NCC-AEAPDMS has the length of 193 ± 0.9 nm and width of 10 ± 0.4 nm, but both samples shared the similar aspect ratio (L/D). This is because TEM only measured the crystalline parts and not the amorphous part.

4. Conclusions

In this work, we have presented that NCC was successfully modified with aminosilane, AEAPDMS, in 80/20 (w/w) water/ethanol solvent which has the potential for CO_2 capture. CHNS results showed that N and C contents increased after the treatment of NCC with AEAPDMS. Meanwhile, the FTIR-ATR analysis revealed that the new peaks for NH_2 bending and wagging as well as Si-CH_3 were determined to show that AEAPDMS was grafted on NCC. The NCC is very crystalline after being hydrolyzed with H_2SO_4; however, after introducing the AEAPDMS on the NCC surface, the crystallinity decreased. This phenomenon was due to the amorphous AEAPDMS that affected the crystalline part in the NCC sample. Nevertheless, the thermal stability of modified NCC remarkably increased since there was interaction between NCC and AEAPDMS. TEM result showed that there was no change in size (nanosize) and shape even after the modification. Moreover, rod-like morphology can be observed in both NCC and NCC-AEAPDMS samples since TEM only detects crystalline part.

Competing Interests

The authors declare that they have no competing interests.

Acknowledgments

The authors would like to thank Universiti Kebangsaan Malaysia and Ministry of Higher Education (MOHE), Malaysia, for providing science fund research grant (03-01-02SF1115), Polymer Research Center (PORCE), and Center for Research Instrumentation and Management (CRIM).

References

[1] A. A. Bakar, A. Hassan, and A. F. Mohd Yusof, "The effect of oil extraction of the oil palm empty fruit bunch on the processability, impact, and flexural properties of PVC-U composites," *International Journal of Polymeric Materials and Polymeric Biomaterials*, vol. 55, no. 9, pp. 627–641, 2006.

[2] F. Fahma, S. Iwamoto, N. Hori, T. Iwata, and A. Takemura, "Isolation, preparation, and characterization of nanofibers from oil palm empty-fruit-bunch (OPEFB)," *Cellulose*, vol. 17, no. 5, pp. 977–985, 2010.

[3] R. Sun, J. M. Fang, L. Mott, and J. Bolton, "Fractional isolation and characterization of polysaccharides from oil palm trunk and empty fruit bunch fibres," *Holzforschung*, vol. 53, no. 3, pp. 253–260, 1999.

[4] M. H. Salehudin, E. Saleh, I. Ida, S. Nur, and H. Mamat, "Cellulose nanofiber isolation and its fabrication into bio-polymer—a review," in *Proceedings of the Conference on Agriculture and Food Engineering International*, 2012.

[5] B. Guo, L. Chang, and K. Xie, "Adsorption of carbon dioxide on activated carbon," *Journal of Natural Gas Chemistry*, vol. 15, no. 3, pp. 223–229, 2006.

[6] S. Kalia, S. Boufi, A. Celli, and S. Kango, "Nanofibrillated cellulose: surface modification and potential applications," *Colloid and Polymer Science*, vol. 292, no. 1, pp. 5–31, 2014.

[7] S. Eyley and W. Thielemans, "Surface modification of cellulose nanocrystals," *Nanoscale*, vol. 6, no. 14, pp. 7764–7779, 2014.

[8] B. L. Peng, N. Dhar, H. L. Liu, and K. C. Tam, "Chemistry and applications of nanocrystalline cellulose and its derivatives: a nanotechnology perspective," *The Canadian Journal of Chemical Engineering*, vol. 89, no. 5, pp. 1191–1206, 2011.

[9] E. Brännvall, *Aspects on strenght delivery and higher utilisation of the strength potential of kraft pulp fibres [Ph.D. thesis]*, Wood Chemistry and Pulp Technology, 2007.

[10] X. Y. B. Eng, *Hydrogels and aerogels based on chemically cross-linked cellulose nanocrystals [Ph.D. thesis]*, McMaster University, Hamilton, Canada, 2014.

[11] C. Salas, T. Nypelö, C. Rodriguez-Abreu, C. Carrillo, and O. J. Rojas, "Nanocellulose properties and applications in colloids and interfaces," *Current Opinion in Colloid & Interface Science*, vol. 19, no. 5, pp. 383–396, 2014.

[12] A. Bendahou, A. Hajlane, A. Dufresne, S. Boufi, and H. Kaddami, "Esterification and amidation for grafting long aliphatic chains on to cellulose nanocrystals: A Comparative Study," *Research on Chemical Intermediates*, vol. 41, no. 7, pp. 4293–4310, 2015.

[13] A. Musa, M. B. Ahmad, M. Z. Hussein, S. Mohd Izham, K. Shameli, and H. Abubakar Sani, "Synthesis of nanocrystalline cellulose stabilized copper nanoparticles," *Journal of Nanomaterials*, vol. 2016, Article ID 2490906, 7 pages, 2016.

[14] N. Lin, J. Huang, P. R. Chang, D. P. Anderson, and J. Yu, "Preparation, modification, and application of starch nanocrystals in nanomaterials: a review," *Journal of Nanomaterials*, vol. 2011, Article ID 573687, 13 pages, 2011.

[15] S. Dong, A. A. Hirani, K. R. Colacino, Y. W. Lee, and M. Roman, "Cytotoxicity and cellular uptake of cellulose nanocrystals," *Nano Life*, vol. 2, no. 3, Article ID 1241006, 2012.

[16] M. Yan, S. Li, M. Zhang, C. Li, F. Dong, and W. Li, "Characterization of surface acetylated nanocrystalline cellulose by single-step method," *BioResources*, vol. 8, no. 4, pp. 6330–6341, 2013.

[17] S. Hokkanen, E. Repo, T. Suopajärvi, H. Liimatainen, J. Niinimaa, and M. Sillanpää, "Adsorption of Ni(II), Cu(II) and Cd(II) from aqueous solutions by amino modified nanostructured microfibrillated cellulose," *Cellulose*, vol. 21, no. 3, pp. 1471–1487, 2014.

[18] S. Kalia, A. Dufresne, B. M. Cherian et al., "Cellulose-based bio- and nanocomposites: a review," *International Journal of Polymer Science*, vol. 2011, Article ID 837875, 35 pages, 2011.

[19] M. Kaushik, C. Fraschini, G. Chauve, J.-L. Putaux, and A. Moores, "Transmission electron microscopy for the characterization of cellulose nanocrystals," in *The Transmission Electron Microscope—Theory and Applications*, K. Maaz, Ed., chapter 6, pp. 129–163, InTech, Rijeka, Croatia, 2015.

[20] A. Hajlane, *Development of hierarchical cellulosic reinforcement for polymer composites [Licentiate thesis]*, Luleå Tekniska Universitet, Luleå, Sweden, 2014.

[21] H. Kargarzadeh, I. Ahmad, I. Abdullah, A. Dufresne, S. Y. Zainudin, and R. M. Sheltami, "Effects of hydrolysis conditions on the morphology, crystallinity, and thermal stability of cellulose nanocrystals extracted from kenaf bast fibers," *Cellulose*, vol. 19, no. 3, pp. 855–866, 2012.

[22] H. Sanaeepur, A. Kargari, and B. Nasernejad, "Aminosilane-functionalization of a nanoporous Y-type zeolite for application in a cellulose acetate based mixed matrix membrane for CO_2 separation," *RSC Advances*, vol. 4, no. 109, pp. 63966–63976, 2014.

[23] C. Gebald, J. A. Wurzbacher, P. Tingaut, T. Zimmermann, and A. Steinfeld, "Amine-based nanofibrillated cellulose as adsorbent for CO_2 capture from air," *Environmental Science & Technology*, vol. 45, no. 20, pp. 9101–9108, 2011.

[24] J. Lu, P. Askeland, and L. T. Drzal, "Surface modification of microfibrillated cellulose for epoxy composite applications," *Polymer*, vol. 49, no. 5, pp. 1285–1296, 2008.

[25] H. Zhang, Y. She, S. Song, H. Chen, and J. Pu, "Improvements of mechanical properties and specular gloss of polyurethane by modified nanocrystalline cellulose," *BioResources*, vol. 7, no. 4, pp. 5190–5199, 2012.

[26] Y. She, H. Zhang, S. Song, Q. Lang, and J. Pu, "Preparation and characterization of waterborne polyurethane modified by nanocrystalline cellulose," *BioResources*, vol. 8, no. 2, pp. 2594–2604, 2013.

[27] N. Ngadi and N. S. Lani, "Extraction and characterization of cellulose from empty fruit bunch (EFB) fiber," *Jurnal Teknologi*, vol. 68, no. 5, pp. 35–39, 2014.

[28] R. M. Sheltami, I. Abdullah, I. Ahmad, A. Dufresne, and H. Kargarzadeh, "Extraction of cellulose nanocrystals from mengkuang leaves (*Pandanus tectorius*)," *Carbohydrate Polymers*, vol. 88, no. 2, pp. 772–779, 2012.

[29] M. Abdelmouleh, S. Boufi, M. N. Belgacem, A. P. Duarte, A. Ben Salah, and A. Gandini, "Modification of cellulosic fibres with functionalised silanes: development of surface properties," *International Journal of Adhesion and Adhesives*, vol. 24, no. 1, pp. 43–54, 2004.

[30] Y. Xie, C. A. S. Hill, Z. Xiao, H. Militz, and C. Mai, "Silane coupling agents used for natural fiber/polymer composites: a review," *Composites Part A: Applied Science and Manufacturing*, vol. 41, no. 7, pp. 806–819, 2010.

[31] L. Segal, J. Creely, A. Martin, and C. Conrad, "An empirical method for estimating the degree of crystallinity of native cellulose using the x-ray diffractometer," *Textile Research Journal*, vol. 29, no. 10, pp. 786–794, 1959.

[32] A. Kumar, Y. S. Negi, V. Choudhary, and N. K. Bhardwaj, "Characterization of cellulose nanocrystals produced by acid-hydrolysis from sugarcane bagasse as agro-waste," *Journal of Materials Physics and Chemistry*, vol. 2, no. 1, pp. 1–8, 2014.

[33] H. Zhao, Y. Ma, J. Tang, J. Hu, and H. Liu, "Influence of the solvent properties on MCM-41 surface modification of aminosilanes," *Journal of Solution Chemistry*, vol. 40, no. 4, pp. 740–749, 2011.

[34] A. Rachini, M. Le Troedec, C. Peyratout, and A. Smith, "Chemical modification of hemp fibers by silane coupling agents," *Journal of Applied Polymer Science*, vol. 123, no. 1, pp. 601–610, 2012.

[35] A. Valadez-Gonzalez, J. M. Cervantes-Uc, R. Olayo, and P. J. Herrera-Franco, "Chemical modification of henequen fibers with an organosilane coupling agent," *Composites Part B: Engineering*, vol. 30, no. 3, pp. 321–331, 1999.

[36] R. Agrawal, N. S. Saxena, K. B. Sharma, S. Thomas, and M. S. Sreekala, "Activation energy and crystallization kinetics of untreated and treated oil palm fibre reinforced phenol formaldehyde composites," *Materials Science and Engineering A*, vol. 277, no. 1-2, pp. 77–82, 2000.

[37] A. Samzadeh-Kermani and N. Esfandiary, "Synthesis and characterization of new biodegradable chitosan/polyvinyl alcohol/cellulose nanocomposite," *Advances in Nanoparticles*, vol. 5, no. 1, pp. 18–26, 2016.

[38] C. Tian, S. Fu, J. Chen, Q. Meng, and L. A. Lucia, "Graft polymerization of epsilon-caprolactone to cellulose nanocrystals and optimization of grafting conditions utilizing a response surface methodology," *Nordic Pulp & Paper Research Journal (NPPRJ)*, vol. 29, no. 1, pp. 58–68, 2014.

[39] M. S. Nazir, B. A. Wahjoedi, A. W. Yussof, and M. A. Abdullah, "Eco-friendly extraction and characterization of cellulose from oil palm empty fruit bunches," *BioResources*, vol. 8, no. 2, 2013.

[40] M. F. Rosa, E. S. Medeiros, J. A. Malmonge et al., "Cellulose nanowhiskers from coconut husk fibers: effect of preparation conditions on their thermal and morphological behavior," *Carbohydrate Polymers*, vol. 81, no. 1, pp. 83–92, 2010.

[41] C. Tian, S. Fu, J. Chen, Q. Meng, and L. A. Lucia, "Graft polymerization of ε-caprolactone to cellulose nanocrystals and optimization of grafting conditions utilizing a response surface methodology," *Nordic Pulp & Paper Research Journal*, vol. 29, no. 1, pp. 58–68, 2014.

[42] H. Zhang, Y. She, X. Zheng, H.-Y. Chen, and J.-W. Pu, "Optical and mechanical properties of polyurethane/surface-modified nanocrystalline cellulose composites," *Chinese Journal of Polymer Science*, vol. 32, no. 10, pp. 1363–1372, 2014.

[43] Y. Wang, B. Tong, S. Hou, M. Li, and C. Shen, "Transcrystallization behavior at the poly (lactic acid)/sisal fibre biocomposite interface," *Composites Part A: Applied Science and Manufacturing*, vol. 42, no. 1, pp. 66–74, 2011.

[44] R. Dash and A. J. Ragauskas, "Synthesis of a novel cellulose nanowhisker-based drug delivery system," *RSC Advances*, vol. 2, no. 8, pp. 3403–3409, 2012.

[45] W. Chen, Q. Li, Y. Wang et al., "Comparative study of aerogels obtained from differently prepared nanocellulose fibers," *ChemSusChem*, vol. 7, no. 1, pp. 154–161, 2014.